



FBMC and UFMC Multi-Waveform Design for 6G Wireless Networks

Zhraa Zuheir Yahya¹, Dia M. Ali^{2*} and Younis Abbosh²

¹Department of Communication Engineering, Ninevah University, Ninevah, Iraq

²Department of Biomedical Engineering, Ninevah University, Ninevah, Iraq

ARTICLE INFO

Article history:

Received November 5, 2024

Revised March 17, 2025

Accepted April 5, 2025

Available online June 1, 2025

Keywords:

5G

6G

FBMC

UFMC

Multi-Waveform

ABSTRACT

The upcoming sixth-generation (6G) mobile is designed with several purposes, such as incredible improvements, ultra-fast speed, ultra-low latency, and massive connections within a small area. Bandwidth Efficiency and extensive coverage, besides sub-millisecond synchronization using a new sub-terahertz spectrum, are also considered. In order to maintain frame consistency, adapt to diverse applications, enable scalability, and minimize interferences, in 6G networks, a multi-waveform architecture is required instead of the individual waveform, which cannot meet the requirements. In this paper, a new approach to the waveform framework is presented. The proposed method integrates multi waveforms, referred to as (Waveforms Interfering). This approach combines two multicarrier schemes within a single frame, and then their performances are independently and collectively checked. The suggested approach has a Power Spectral Density (PSD) with minimal out-of-band radiation (OOBR) and a reduced guard band to 6 subcarriers between the two waveforms without causing interference. The Bit Error Rates (BER) performance compared among different orders of Quadrature Amplitude Modulation (QAM). The minimum BER achieved at 20dB SNR is $9e^{-7}$. This comparison reveals diverse performance outcomes based on the modulation orders used. The Peak Average Power Ratio (PAPR) behaves similarly to an individual scheme. This approach can effectively satisfy the strict performance requirements of 6G networks.

1. Introduction

Each mobile generation of communication system expands the number of adjustable parameters to meet specific requirements as needed [1]. In contrast, sixth-generation (6G) will encounter a broader range of demands than fifth-generation (5G). New air interface and transmission techniques are required for higher bandwidth and improved energy efficiency. The 6G conceptual framework envisages universal coverage, spanning all spectrums, fully accommodating varying applications, and ensuring strong defenses against hackers and other unauthorized users [2]. One crucial consideration for each generation's evolution is

waveform design in the physical layer [3]. In the Fourth Generation (4G), the waveform used was Orthogonal Frequency Division Multiplexing (OFDM), which has some limitations. With the emergence of 5G, more advanced OFDM waveforms have been proposed with additional attributes while maintaining the benefits inherited from their predecessors [4].

Moving towards 6G, identical underlying multicarrier waveforms will be adopted, although they may be refined further [5]. This will allow future development in 6G standards that will unify the system for multiple applications, thereby increasing the throughput capacity. This approach is projected to lead to a

* Corresponding author.

E-mail address: dia.ali@uoninevah.edu.iq

DOI: [10.24237/djes.2024.18202](https://doi.org/10.24237/djes.2024.18202)

This work is licensed under a [Creative Commons Attribution 4.0 International License](https://creativecommons.org/licenses/by/4.0/).



potential escalation of parameters and numerologies that must be configured for a singular waveform [6]. The 6G vision, in terms of standards, involves employing multiple dissimilar waveforms within a single frame, where each waveform has different numerological attributes. In addition, "inter waveform interference" is a novel type of interference that would need sophisticated control through a new waveform processing paradigm [3]. This integration of multi-waveforms is expected to enhance the flexibility of each waveform by having potentially more diverse numerology structures per waveform [7-8]. 6G can assign waveforms with varying parameter profiles to users using Machine Learning (ML) techniques. Adopting ML techniques for integration optimization in communication networks has been applied in the 6G network, which represents development at the physical layer level [9-10].

Maintaining frame consistency and meeting the diverse application demands in 6G networks remain critical challenges. Current studies have primarily focused on single-waveform designs. However, these approaches face limitations. Such limits include a lack of flexibility for heterogeneous applications, limited scalability, and frame consistency [11]. The most well-known waveforms identified over 5G and beyond are filtered-OFDM (F-OFDM), Universal Filter Multicarrier (UFMC), Filter Bank Multicarrier (FBMC), and Generalized Frequency Division Multiplexing (GFDM). Each waveform has its own specifications and performance characteristics. UFMC applies a filter per each sub-band, providing a balance between the spectrum efficiency and computational complexity. UFMC can be used for diverse services, as well as high-speed broadband and low-latency applications. UFMC is not suitable for higher data rate applications [12]. Under F-OFDM, the designated spectrum is divided into narrower sub-bands, each containing its own modulated subcarriers. The main limitation of F-OFDM is low energy efficiency due to the high Peak to Average Power Ratio (PAPR) [13]. In the FBMC, every filter bank performs independent filtering at each carrier. Notably, this sophisticated filtering

architecture boasts better spectrum efficiency than its counterparts. Despite its advantages, it causes an increase in complexity and time delay, making it unsuitable for applications that require less implementation latency [13-15]. GFDM, on the other hand, is a block-oriented modulation scheme that uses subcarriers at close ends, pulse shaping to reduce inter-carrier interference (ICI), and ensures that the addition of spectrum confinement Cyclic prefix (CP) reduces the effect of Inter-Symbol Interference (ISI) again. The main limitation of GFDM is its complexity in design and processing. A detailed overview of the 5G waveforms and subsequent generation is provided in [16].

In 6G, multi-waveform approaches are adopted to tackle the diverse and dynamic requirements of emerging applications. Each waveform succeeds in specific scenarios, such as high data rate, low latency, or energy efficiency, but none can meet all requirements simultaneously. Multi-waveform architecture offers flexibility, allowing the selection or combination of waveforms to optimize performance based on application needs, environment conditions, and user requirements, ensuring enhanced spectral efficiency, robustness, and adaptability. The concept of combining more than two waveforms in a joint design is to pursue optimal performance, revealing superior advantages compared to a single waveform. This study starts with this concept by forming two different waveforms and then integrating them into a communication system to evaluate their performance in the upcoming 6G environment.

The remainder of this paper is organized as follows: Section 2 provides an overview of the prior research encompassing FBMC and UFMC schemes. Moving forward, Section 3 delineates the proposed architecture along with the block diagram detailing the multi-waveform configuration. In Section 4, a comprehensive exploration of the signal preparation for multi-waveform design is provided. Subsequently, Section 5 shows the results obtained and discusses them, while conclusions in Section 6.

2. Related work

In [17], an investigation into the efficacy of pulse shaping-based FBMC modulation techniques in 5G mobile communication systems was presented. The results obtained from simulations demonstrate that the FBMC system surpasses the conventional OFDM system in terms of spectrum efficiency and other critical parameters. These parameters included the attainable channel capacity, signal-to-noise ratio (SNR), temporal and spectral responses, and the extent of out-of-band signal leakage. In [18], the authors introduced a method for designing compact filters with minimal undesirable spectral emissions through optimization. Simulation results indicated that the filters designed using this approach outperform existing short filters, displaying superior performance characteristics. In [19], the authors employed an optimization method based on Selective Mapping (SLM) to enhance the performance of UFMC-PAPR. This study introduced one of the Crow Search Algorithms (CSA), an innovative heuristic optimization technique inspired by the cognitive behavior of crows, for optimizing SLM. The proposed method was a radical departure from the standard UFMC, the SLM-UFMC system, and SLM-UFMC with conventional optimization techniques. In [20], the authors presented a new approach to designing an efficient QAM-FBMC filter with a short length. This novel design was focused on reducing overall interference seen at the receiver side.

During the development of the prototype filter, the authors carefully probed and optimized total interference with and without channel effects. Performance results suggest that filters designed in this work perform better than QMF, NPR, and Gaussian filters. Similarly, in [21], a detailed analysis of GFDM and UFMC waveforms based on several time domain windowing techniques is presented. Simulation results, which include BER evaluations and PAPR, favor the hamming window over Dolph-Chebyshev and Kaiser. The authors in [22] proposed combining waveforms using three distinct architectures (OFDM, FBMC, and UFMC). Through hardware virtualization,

dynamic adjustments were enabled to enhance the throughput and achieve a significant power reduction of up to 88%. In another context, [23] proposed using the UFMC waveform for radar and communication systems. This waveform exhibited the capacity to serve these applications with a manageable level of complexity, offering optimal Spectrum efficiency. The authors in [24] focused on the design nuances of UFMC with varying numerological considerations. The work confirmed that BER and CCDF performance were affected by different filter lengths and modulation schemes. Also, in [25], the authors used FBMC technology, clamming better performance than conventional OFDM in various metrics such as BER, maximum power, PSD, noise-PSD, power and magnitude, and phase responsiveness. They also discussed the advantages of FBMC technology over OFDM and spectrum performance. In [26], an innovative approach focused on orthant optimization technology is used to design optimal filters for FBMC systems under next-generation smart e-healthcare network architecture. This effort achieved high spectral efficiency, at the expense of significant guard band frequencies, to accommodate real-time e-health networks. The authors in [27] outlined the development and evaluation of algorithms to enhance FBMC and OQAM auto interference compensation in MIMO networks with memory. Through simulation, modeling, and performance comparison, algorithms showed equivalent performance in terms of the bit error rate (BER) and error vector magnitude with solutions with similar computational complexity; a similar level of performance was shown compared to a more complex parallel multistage algorithm. They conducted a study on FBMC and UFMC and included communication systems shared to monitor the performance of 6G applications. This study cleverly designed multi-waveform architecture that organizes mathematical overlaps and introduces a new type of inter-waveform interference (IWI). In [28], the authors use the Tukey filtering technique to enhance the UFMC performance and reduce the complexity. Simulation results show a decrease in PAPR and

enhancement in BER compared to conventional UFMC.

Unlike most of the previous studies, our method involved a specialized architecture to manage the integration of the two waveforms,

focusing on spectral efficiency and interference minimization. Table 1 highlights the differences and advantages of our work compared with previous studies.

Table 1: Comparison among previous studies

Aspect	Previous studies	This work
Waveform performance enhancement	[17], [21] and [22] focused on designing or improving the performance of a single waveform (UFMC, FBMC, and GFDM)	Introduces a system that integrates two waveforms (UFMC and FBMC) to handle diverse data types
Enhancing single waveform reliability	[19] and [26] use techniques such as optimized filter designs to improve the reliability of single waveform	High-priority data is directed to the FBMC branch for its superior spectral efficiency, while non-critical data is routed to the UFMC branch, improving the overall system performance.
UFMC in specific applications	[23] focus on UFMC in specific contexts (radar or multi-access)	Evaluate the performance of the proposed system under different channels, including Additive White Gaussian Noise (AWGN), with plans to extend to multipath channels in future work
Performance optimization for specific environments	[20] and [24] optimized performance for specific environments or applications	Offers high flexibility by combining two waveforms that support diverse applications

3. Multi-Waveform

The main idea of the proposed approach is to combine two different waveforms with different data types. The first data type is, for example, low-speed, low-reliability information directed to the UFMC branch. UFMC is well-suited for handling delay-tolerant due to its low complexity and flexibility in handling fragmented spectrum resources. High data rate and reliable information directed to the FBMC waveforms branch for more robustness and superior spectral efficiency. Each waveform is loaded with specific information seamlessly into a combined waveform. This scenario was chosen to ensure the flexibility and adaptability to various application demands of 6G networks. Figure 1 visually covers the power spectrum structure of the internal convergence of the proposed waveform.

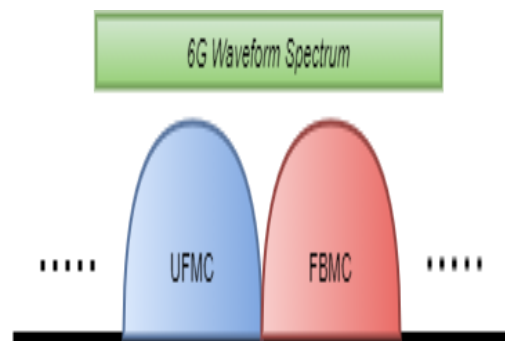


Figure 1. Spectrum of proposed multi-waveform

Figure 2 shows the combination of the new waveform in which the individual data and waveforms are generated independently, and the resulting signals are combined prior to transmission and submitted to background channel characteristics. At the first path of the transmitter side, the UFMC signal is carefully tuned in each sub-band. The generated data is modulated by Quadrature Amplitude modulation (QAM). The processed data is then subjected to an Inverse Fast Fourier Transform (IFFT) to prepare it for transmission. Sub-band

refinement is achieved by applying a Dolph-Chebyshev filter. Zero Prefix (ZP) is added to the filtered signal to prevent interferences due to the multipath channel.

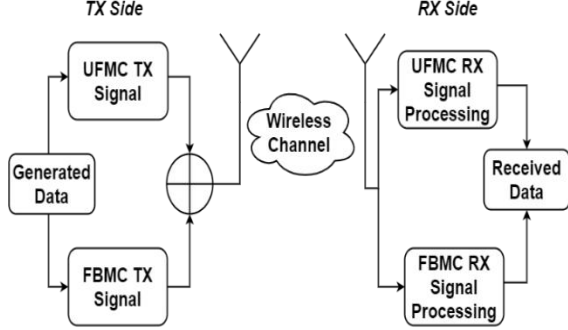


Figure 2. Proposed multi-waveform block diagram

For the second path of the transmitter, FBMC data is modulated using Offset QAM to reduce ISI caused by pulse shape. Then, the updated signals are converted from a sequential system to a parallel system to perform modulated signal filtering followed by data reconstruction, which comes sequentially in parallel form. Finally, the FBMC and UFMC signals are combined and transmitted.

The received signal in the reception front end goes through two processing stages. The critical step for the UFMC signal involves its passage through time domain windowing, which is strategically applied to combat the negative effects of ISI. This is followed by a 2N-point fast Fourier transform (FFT), where 'N' is the number of subcarriers. The opposite process of the Rx filter is introduced to overcome the distortions due to the filter on the transmitter side. Then, a QAM demodulator is used to extract the original data bits.

In the context of FBMC, the received signals assume a parallel configuration, paving the way for applying the filterbank process (PPN and FFT). After this, data is transformed into a parallel format, and demodulation through Offset Quadrature Amplitude Modulation (OQAM) transpires to recover the received bits. The specific procedural workflows for individual UFMC and FBMC operations are delineated in Figure 3 and Figure 4, respectively.

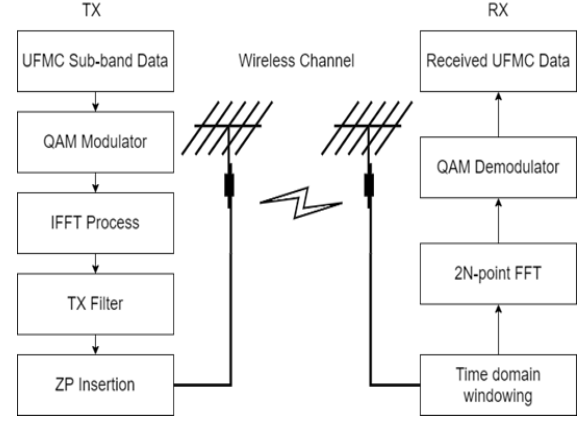


Figure 3. UFMC process

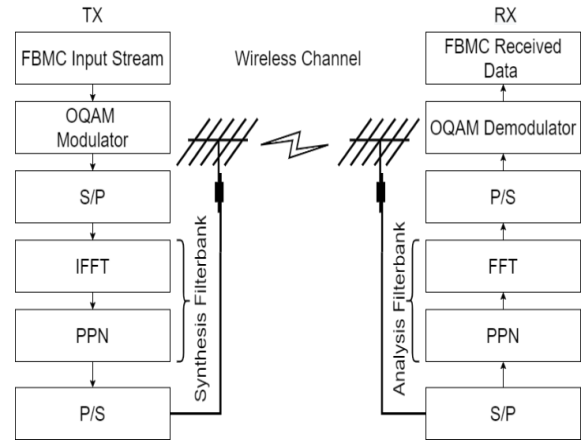


Figure 4. FBMC process

4. Multi-Waveform Signal

4.1 Multi-Waveform Signal Preparation

At the transmitter, the prepared UFMC signal from m^{th} users can be expressed as:

$$S^{UFMC} = \sum_{i=0}^{N_B} S_i^m(n) \quad 0 < n < N + L - 1 \quad (1)$$

where N_B denotes the maximum sub-band number and $S_i^m(n)$ is the sub-band signal, which can be expressed as:

$$S_i^m(n) = \sum_{l=0}^{L-1} f_i(l) x_i^m(n-l) \quad 0 < n < N + L - 1 \quad (2)$$

Where $f_i(l)$ is the coefficient of the l^{th} filter and can be expressed as:

$$f_i(l) = f(l) e^{\frac{j2\pi lc_i}{N}} \quad 0 < l < L - 1 \quad (3)$$

where c_i is the index of the center subcarrier for the i^{th} sub-band, and x_i^m is the output of IFFT and expressed as:

$$x_i^m(n) = \frac{1}{N} \sum_{k \in B_i^m} X_i^m(k) e^{\frac{j2\pi kn}{N}} \quad 0 < n < N - 1 \quad (4)$$

$X_i^m(k)$ is the complex data symbol relating to the m^{th} user's sub-band, and B_i^m is the sub-band assigned to the m^{th} user [15].

For FBMC, the FBMC-OQAM signal can be expressed as:

$$s^{FBMC}(n) = \sum_{s \in Z} \sum_{i \in I} X_{i,s} \theta_{i,s} P_i \left[n - s \frac{N}{2} \right] \quad (5)$$

where I contain indices of the active subcarriers, and N is the total number of subcarriers.

$X_{i,s}$ is the modulated symbol of the subcarrier i and the FBMC symbol time index s . $\theta_{i,s}$ is the phase rotation linked to the OQAM mapping. $P_i[n]$ is the filter for subcarrier i . the length of filter $L=KN$. K is the overlapping factor of the FBMC symbols.

$$P_i(n) = P(n)e^{j\frac{2\pi mn}{M}} \quad (6)$$

Where $P(n)$ is the prototype filter and the exponential factor corresponds to the m^{th} subcarrier.

The total transmitted signal $s_T(n)$ of the proposed design is the combination of the UFMC signal and FBMC signal, which can be expressed as:

$$s_T(n) = s^{UFMC}(n) + s^{FBMC}(n) \quad (7)$$

The transmitted signal ($X_{m,k}$) on the AWGN channel can be expressed as:

$$X_{m,k} = \sum s_T(n) + w_i(n) \quad (8)$$

Where a $w_i(n)$ is the AWGN, and w_i is the corresponding user, which is allocated at the i th sub-band.

4.2 Computational complexity

The overall transceiver complexity for multi-waveform combines the complexities of both UFMC and FBMC. UFMC involves filtering at each sub-band; the complexity of the filter of length L and overlap factor I_{UFMC} can be calculated:

$$C_{UFMC \text{ Filter}} = I_{UFMC}(N_s N + N_{ZP}) \quad (9)$$

where N_s is the number of symbols, N is FFT size, and N_{ZP} is the zero prefix length.

FFT complexity can be calculated as follows:

$$C_{UFMC \text{ FFT}} = 3N_s N \log_2(N_s N) + 4N_s N \quad (10)$$

The total UFMC complexity can be expressed as:

$$C_{UFMC} = 3N_s N \log_2(N_s N) + 4N_s N + 2I_{UFMC}(N_s N + N_{ZP}) \quad (11)$$

FBMC uses filtering per sub-carrier with overlapping symbols, thus increasing the computational cost compared to UFMC. The prototype filter complexity is:

$$C_{FBMC \text{ Filter}} = K \cdot N \cdot N_s \quad (12)$$

FFT complexity is similar to that in UFMC. Total FBMC complexity can be expressed as:

$$C_{FBMC} = 3N_s N \log_2(N_s N) + 4N_s N + K \cdot N \cdot N_s \quad (13)$$

Multi-waveform complexity can be expressed as:

$$C_{\text{Multi-waveform}} = \alpha \cdot C_{UFMC} + (1 - \alpha)C_{FBMC} \quad (14)$$

where α represents the fraction of data processed.

Table 2 compares the processing power, power consumption, and computational requirements of UFMC, FBMC, and multi-waveform systems. It outlines how the computational complexity and power consumption vary for each system, with UFMC being less resource-intensive than FBMC but FMBC offering higher spectral efficiency at the cost of increased complexity and power demand. Additionally, the table highlights the trade-offs in multi-waveform systems, which combine the strengths of both the UFMC and FBMC but require significantly more processing power and result in higher energy consumption. The table also points out the challenge of battery-powered applications.

Table 2: Comparison of computational complexity and power consumption for UPMC, FBMC, and multi-waveform

Waveform	Processing power for filtering, modulation, and demodulation	Power consumption
UPMC	-Filtering for each sub-band. The complexity depends on the number of symbols N_s and FFT size N . -Modulation and demodulation: require FFT/IFFT operations, with complexity increasing with the number of symbols and FFT.	Lower power consumption compared to FBMC due to less complex filtering.
FBMC	-Filtering for each subcarrier with overlapping symbols increases complexity compared to UPMC. - Modulation and demodulation: require FFT/IFFT operations, with complexity increasing with the number of symbols and FFT	Higher power consumption compared to UPMC and lower than multi-waveform
Multi-waveform	Higher computational complexity, Higher flexibility, and spectral efficiency	Increased power consumption is due to the combination of both waveforms. Battery usage: Mobile may face challenges in battery life due to the increased power consumption

4.3 Inter-Waveform-Interference

If $g_{UPMC}(t)$ and $g_{FBMC}(t)$ are the impulse responses of UPMC and FBMC filters, respectively, then the interference signal characterizes the inter-waveform-interference can be represented as:

$$I_s = g_{UPMC}(t) - g_{FBMC}(t) \quad (15)$$

The cross-interference $I_{UPMC-FBMC}$ measures how the UPMC filter interacts with the FBMC in the overlapping frequency range. Ideally, this value should be minimized to reduce the inter-waveform interference.

$$I_{UPMC-FBMC} = \int_{-\infty}^{\infty} g_{UPMC}(t)g_{FBMC}^*(t) \quad (16)$$

5. Simulation results

Based on the proposed block diagram shown in Figure 2, MATLAB simulates each block with its respective parameter. The main parameters for simulation are listed in Table 3.

These parameters are chosen to optimize system performance for specific applications or scenarios. Altering these parameters would significantly affect the trade-offs between spectral efficiency, robustness, complexity, and

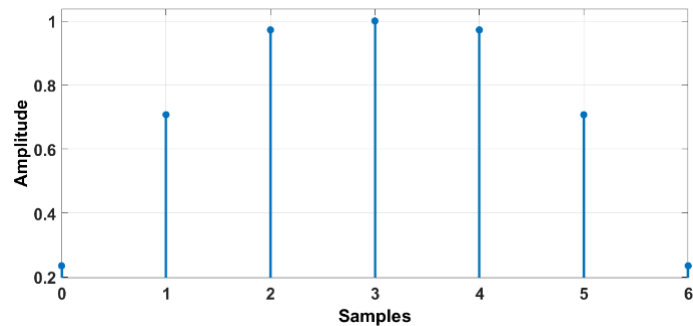
latency, providing insight into waveform adaptability and applications-specific performance.

Figure 5 visualizes the impulse response characterizing the designed filters. The UPMC configuration encompasses a solitary sub-band housing a total of 200 subcarriers. In this context, the Chebyshev filter takes precedence. In the realm of FBMC, the signal is architected with a factor 'K' equating to 4, encompassing a subcarrier count of 60. The harmonious fusion of these two distinct waveforms culminates in their joint transmission over an AWGN channel.

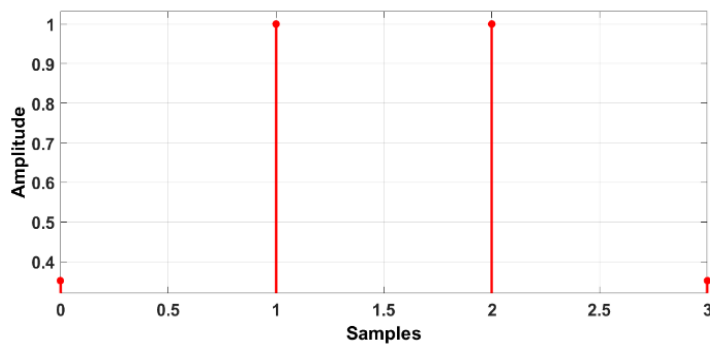
Figure 6 provides a visual representation of the PSD of the combined waveforms, showcasing the attainment of a minimal guard band while effectively evading interference. Each waveform uniquely presents distinct OOB profiles, where the sidelobe attenuation achieved in UPMC using the Chebyshev filter and FBMC are -30 dB and -80 dB, respectively, facilitating diverse service provisions. Due to these values, the band of each waveform is moved toward the other until the minimized guard band is achieved. A lower value achieved is six subcarriers, where no interference occurs.

Table 3: Simulation parameters

Parameter	Setting	Reason
UFMC FFT size	1024	For broader bandwidth.
FBMC FFT size	512	For higher efficiency over a narrower bandwidth.
Data subcarrier	200	To ensure a balance between throughput and spectral efficiency.
Filter type	Prototype	Offer sharp transition band and support evaluation under various conditions.
Window type	Dolph-Chebyshev	Provides steep spectral roll-offs.
QAM level	16, 64, 128, 256	This is for assessing performance under different spectral efficiency and robustness trade-offs.
Filter length	4 for UFMC and 7 for FBMC	To reduce computational complexity and latency, enhances spectral confinement and efficiency.



(a)



(b)

Figure 5. The impulse response of the utilized filters (a) FBMC, (b) UFMC

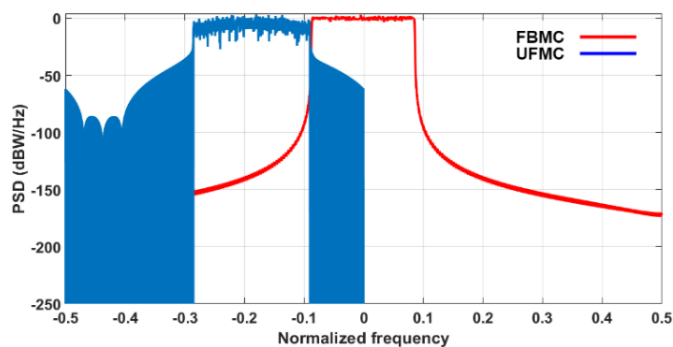


Figure 6. PSD of the designed multi-waveform

The evaluation of the novel waveform design entails a comprehensive analysis of BER and PAPR. As depicted in Figure 7, the BER performance consistently decreases with increasing SNR, allowing for a direct

comparison with the individual waveforms. The discernible outcome reveals that the proposed design aligns closely with the performance profiles of UPMC and FBMC waveforms, where at SNR=20 dB, the BER achieved is $9e^{-7}$.

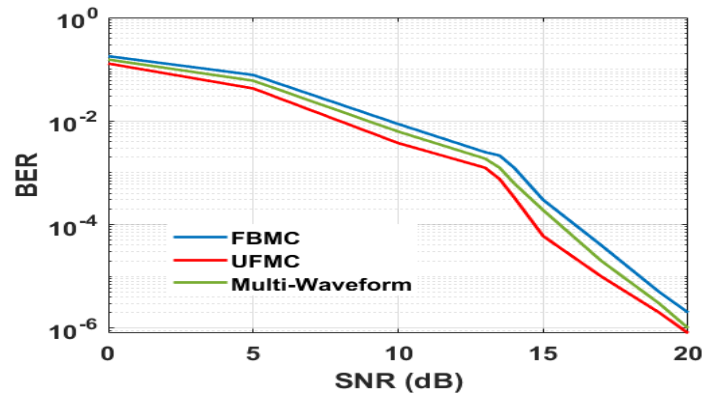


Figure 7. BER Comparison among the proposed design

The average BER of the proposed architectural design is juxtaposed across a range of QAM levels. As depicted in Figure 8, the BER performance is depicted under varying SNR conditions. Notably, it becomes evident that the BER curves exhibit degradation as QAM levels escalate, especially when

contrasted with lower modulation levels. Furthermore, the utilization of higher QAM levels necessitates the incorporation of a more expansive guard band to maintain isolation between the spectrums of the individual waveforms.

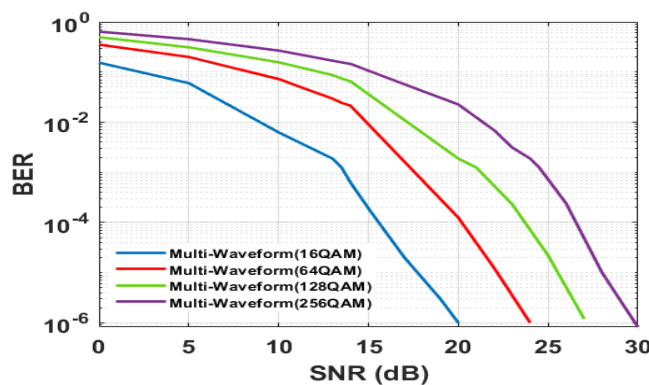


Figure 8. Proposed design BER comparison for various QAM levels

For the FBMC and UPMC, the constellation diagrams of the received symbols are meticulously juxtaposed against the corresponding transmitted symbols, as vividly showcased in Figure 9(a), (b), (c), and (d) for 16,

64, 128, and 256 QAM levels. The received constellation points are inherently aligned with the form exhibited by their transmitted counterparts.

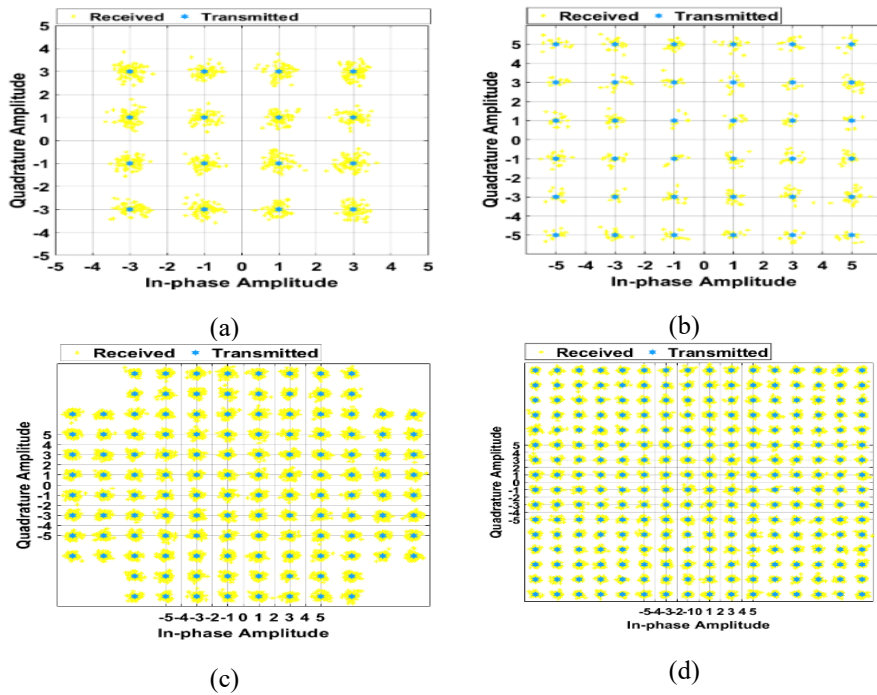


Figure 9. Transmitted and received constellation points (a) 16-QAM (b) 64-QAM (c) 128-QAM (d) 256-QAM

Figure 10 undertakes a comparative analysis, pitting the proposed multi-waveform's performance against that of FBMC and UFMC in the context of PAPR. The UFMC exhibits slightly higher values than the FBMC. This is

due to the windowing effect applied in FBMC, which effectively smooths out the power peaks across the subcarrier. However, the combined waveform maintains a balanced trade-off by leveraging the strength of both approaches.

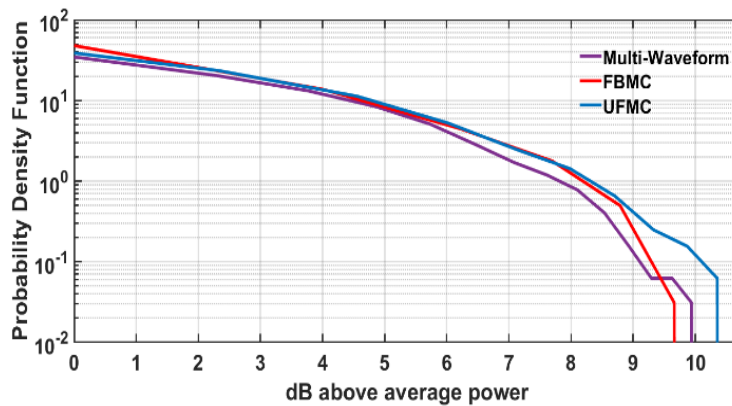


Figure 10. PAPR of the proposed multi-waveform

Figure 11 shows the sampled time points corresponding to the UFMC filter, FBMC signal, and interference signal. The UFMC filter achieves a smooth transition and symmetric shape, which is consistent with Chebyshev filter characteristics. The amplitude peaks in the middle time samples, indicating its focus on maintaining energy concentration over the defined period. The FBMC filter values vary

dynamically, especially toward the end samples. The amplitude difference between UFMC and FBMC filters is apparent, especially at the edges. The interference signal shows significant values where the two filters differ, particularly at the boundaries. The peak interference at time = 2 highlights the mismatch between the filters regarding sidelobe attenuation or design characteristics.

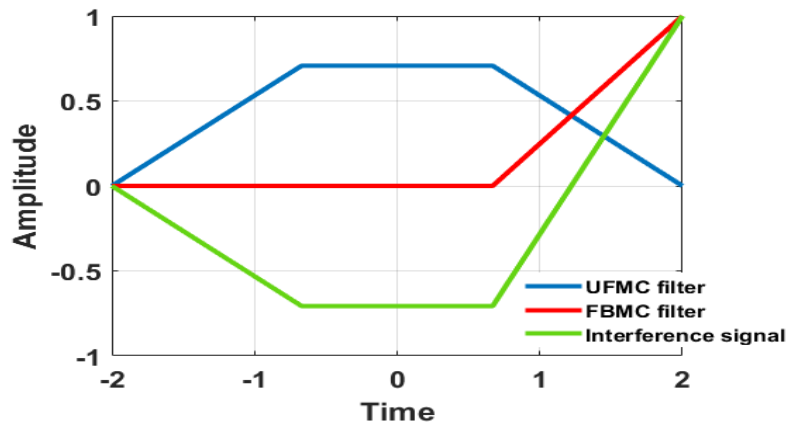


Figure 11. UFMC and FBMC filters, along with interference signal

6. Conclusions

A multi-waveform architecture is proposed in this paper instead of the individual waveform to maintain frame consistency, adapt to diverse applications, enable scalability, and minimize the interferences for 6G communication systems. FBMC and UFMC, two distinct multicarrier waveforms, were seamlessly integrated with different numerical attributes. Simulation results in terms of BER show that the proposed approach aligns closely with the performance of UFMC and FBMC, where at SNR=20 dB, the BER achieved is $9e^{-7}$. The PSD of the proposed design yielded advantages like reduced OOB and a narrower guard band of about six subcarriers between the two waveforms. Moreover, a BER comparison across varying QAM levels disclosed that higher levels incurred worsened performance. Regarding PAPR, the proposed design maintains a balanced trade-off by leveraging the strength of both UFMC and FBMC. The proposed approach combines the complexities of both UFMC (moderate) and FBMC (moderate) depending on the data allocation strategy, which slightly has higher complexity. The trade-off lies in performance improvement and computational overhead. This novel approach promises a solution that allows flexible selection of waveform for specific

application requirements, reduces interference, enables scalability, and maintains frame consistency for reliable communications. In future works, the issue of power consumption will be addressed.

References

- [1] M. Banafaa, et al., "6G Mobile Communication Technology: Requirements, Targets, Applications, Challenges, Advantages, and Opportunities," *Alexandria Engineering Journal*, vol. 64, pp. 245–274, Feb 2023. DOI: [10.1016/j.aej.2022.08.017]
- [2] Y. Xiaohu et al., "Towards 6G wireless communication networks: vision, enabling technologies, and new paradigm shifts," *Science China Information Sciences*, vol. 64, no. 1, pp. 1–74, Jan 2021. DOI: [10.1007/s11432-020-2955-6]
- [3] Y. Ahmet and A. Hüseyin, "A Waveform Parameter Assignment Framework for 6G With the Role of Machine Learning," *IEEE Open Journal of Vehicular Technology*, vol. 1, pp. 156–172, May 2020. DOI: [10.1109/OJVT.2020.2992463]
- [4] O. M. Salih and A. I. Siddiq, "A Low Complexity SLM Scheme for Papr Reduction of OFDM Signals", *DJES*, vol. 10, no. 3, pp. 63–74, Sep 2017. DOI: [10.24237/djes.2017.10306](https://doi.org/10.24237/djes.2017.10306)
- [5] H. Tataria et al., "6G Wireless Systems: Vision, Requirements, Challenges, Insights, and Opportunities," *Proceedings of the IEEE*, vol. 109, no. 7, pp. 1166–1199, May 2021. DOI: [10.1109/JPROC.2021.3061701]
- [6] Asghar et al., "Evolution of Wireless Communication to 6G: Potential Applications and Research Directions," *Sustainability*, vol. 14, no. 10, p. 6356, May 2022. DOI: [10.3390/su14106356]

- [7] A. Dogra et al., "A Survey on Beyond 5G Network With the Advent of 6G: Architecture and Emerging Technologies," *IEEE Access*, vol. 9, Oct 2020, pp. 67512–67547. DOI: [10.1109/ACCESS.2020.3025710]
- [8] A. Yazar et al., "6G vision: An ultra-flexible perspective," *ITU Journal on Future and Evolving Technologies*, vol. 1, no. 1, pp. 121–40, Dec 2020. DOI: [10.52953/ILVJ2571]
- [9] A. M. Ahmed, S. A. Majeed, and S. A. Hasan, "Non-Terrestrial Networks Based on Non-Orthogonal Multiple Access Towards 6G", *DJES*, vol. 17, no. 2, pp. 1–26, Jun. 2024. DOI: [10.24237/djes.2024.17201](https://doi.org/10.24237/djes.2024.17201)
- [10] A. M. Ahmed, S. A. Majeed, and Y. S. Dawood, "A Survey of 6G Mobile Systems, Enabling Technologies, and Challenges," *International Journal of Electrical and Electronic Engineering & Telecommunications*, vol. 12, no. 1, Jan 2023. doi: 10.18178/ijeetc.12.1.1-21
- [11] Yazar, Ahmet, et al. "6G Vision: An Ultra-Flexible Radio Access Technology Perspective." *arXiv: Signal Processing (2020)*: n. pag.
- [12] Dia M. Ali and Zhrraa Zuheir Yahya, "5G F-OFDM Waveform Based Software-Defined Radio Technology," *Proceedings of Engineering and Technology Innovation*, vol. 20, pp. 68–80, Jan 2022. DOI: [10.46604/peti.2022.8887](https://doi.org/10.46604/peti.2022.8887)
- [13] M. S. Noorzilina, S. M. Sulong, A. Idris, M. S. M. Said, I. Ahmad, "Design of MIMO F-OFDM System Model for PAPR Reduction in the Growth of 5G Network", *Journal of Physics. Conference Series (Online)*, vol. 1793, no. 1, p.7, Feb. 2021. doi: 10.1088/1742-6596/1793/1/012067.
- [14] Dia M. Ali and Zhrraa Zuheir Yahya, "Flexible Subbands F-OFDM Configured for Spectrum Efficiency Enhancement in 5G System," *Journal of Communications*, vol. 17, no. 3, pp. 203–209, Mar 2022. doi:10.12720/jcm.17.3.203-209
- [15] Dia M Ali, Zhrraa Zuheir Yahya, and Younis M Abbosh, "OTFS Waveform Effectiveness in 6G Communication Networks," *International Journal of Microwave and Optical Technology*, vol. 18, no. 1, pp. 1–6, Jan 2023.
- [16] A. Adoum, et al., "A Comprehensive Survey of Candidate Waveforms for 5G, beyond 5G and 6G Wireless Communication Systems," *Open Journal of Applied Sciences*, vol. 13, no. 1, pp. 136–61, Jan 2023.
- [17] S. P. Yadav, "Filter Bank Multicarrier Modulation Techniques for 5G and Beyond Wireless Communication Systems," *European Journal of Electrical Engineering and Computer Science*, vol. 6, no. 2, pp.18–24, Mar 2022. DOI:[10.24018/ejece.2022.6.2.423](https://doi.org/10.24018/ejece.2022.6.2.423)
- [18] I. Galdino et al., "Short Prototype Filter Design for OQAM-FBMC Modulation," *IEEE Transactions on Vehicular Technology*, vol. 69, no. 8, pp. 9163–9167, Jun 2020. DOI: [10.1109/TVT.2020.2992463]
- [19] A. Madhusudhan and S. K. Sharma, "Selective mapping scheme for universal filtered multicarrier," *Intelligent Automation & Soft Computing*, vol. 36, no.2, pp. 1273–1282, Jan 2023. DOI: [10.32604/iasc.2023.030765](https://doi.org/10.32604/iasc.2023.030765)
- [20] I. Galdino Andrade et al., "Short-Filter Design for Intrinsic Interference Reduction in QAM-FBMC Modulation," *IEEE Communication Letters*, vol. 24, no. 7, pp. 1487–1491, Mar 2020. DOI: [10.1109/LCOMM.2020.2992463]
- [21] M. Gupta et al., "Comparative Study on Implementation Performance Analysis of Simulink Models of Cognitive Radio Based GFDM and UFMC Techniques for 5G Wireless Communication," *Wireless Personal Communications*, vol. 126, pp. 1–31, Sep 2020. DOI: [10.1007/s11277-020-07788-1]
- [22] F. M. Lopes, and J. C. Ferreira, "Flexible Baseband Modulator Architecture for Multi-Waveform 5G Communications," *Field Programmable Gate Arrays (FPGAs) II*, 1st ed., IntechOpen, 2020, ch. 3. [Online]. Available: <https://www.intechopen.com/books/8360>.
- [23] K. Imane et al., "UFMC Waveform and Multiple-Access Techniques for 5G RadCom," *Electronics*, vol. 10, no. 7, p. 849, Apr 2021. DOI: [10.3390/electronics10070849]
- [24] S. Lambros et al., "5G UFMC Scheme Performance with Different Numerologies" *Electronics*, vol. 10, no. 16, p. 1915, Aug 2021. DOI: [10.3390/electronics10161915]
- [25] B. Ramakrishnan et al., "Analysis of FBMC Waveform for 5G Network Based Smart Hospitals," *Applied Sciences*, vol. 11, no. 19, p. 8895, Sep 2021. DOI: [10.3390/app11198895]
- [26] A. Adarsh et al., "Low-latency and High-Reliability FBMC Modulation scheme using Optimized Filter design for enabling NextG Real-time Smart Healthcare Applications," *The Journal of Supercomputing*, vol. 79, pp. 3643–3665, Mar 2023. DOI: [10.1007/s11227-023-05123-4]
- [27] V. O. Varlamov et al., "Investigation of FBMC-OQAM Equalization with Real Interference Prediction Algorithm Properties for MIMO Transmission Scheme," *Sensors*, vol. 23, no. 4, p. 2111, Feb 2023. DOI: [10.3390/s23042111]
- [28] S. Debnath, S. Ahmed, S. S. Alam, "Analysis of filtered multicarrier modulation techniques using different windows for 5G and beyond wireless systems," *Wireless Communications and Mobile Computing*, vol. 2024, no 1, p. 9428292, Mar 2024. DOI: [10.1155/2024/9428292]